Advances in Aircraft and Spacecraft Science, *Vol. 6, No. 2 (2019) 145-156*
DOI: https://doi.org/10.12989/aas.2019.6.2.145

Creating damage tolerant intersections in composite structures using tufting and 3D woven connectors

Harry M. Clegg*[1], Giuseppe Dell'Anno[1a] and Ivana K. Partridge[2b]

[1]*The National Composites Centre, Bristol & Bath Science Park, Bristol, United Kingdom*
[2]*Bristol Composites Institute, The University of Bristol, Bristol, United Kingdom*

(Received October 15, 2018, Revised December 21, 2018, Accepted January 3, 2018)

Abstract. As the industrial desire for a step change in productivity within the manufacture of composite structures increases, so does the interest in Through-Thickness Reinforcement technologies. As manufacturers look to increase the production rate, whilst reducing cost, Through-Thickness Reinforcement technologies represent valid methods to reinforce structural joints, as well as providing a potential alternative to mechanical fastening and bolting. The use of tufting promises to resolve the typically low delamination resistance, which is necessary when it comes to creating intersections within complex composite structures. Emerging methods include the use of 3D woven connectors, and orthogonally intersecting fibre packs, with the components secured by the selective insertion of microfasteners in the form of tufts. Intersections of this type are prevalent in aeronautical applications, as a typical connection to be found in aircraft wing structures, and their intersections with the composite skin and other structural elements. The common practice is to create back-to-back composite "L's", or to utilise a machined metallic connector, mechanically fastened to the remainder of the structure. 3D woven connectors and selective Through-Thickness Reinforcement promise to increase the ultimate load that the structure can bear, whilst reducing manufacturing complexity, increasing the load carrying capability and facilitating the automated production of parts of the composite structure. This paper provides an overview of the currently available methods for creating intersections within composite structures and compares them to alternatives involving the use of 3D woven connectors, and the application of selective Through-Thickness Reinforcement for enhanced damage tolerance. The use of tufts is investigated, and their effect on the load carrying ability of the structure is examined. The results of mechanical tests are presented for each of the methods described, and their failure characteristics examined.

Keywords: dry-fibre; T-joints; TTR; tufting; 3D woven; damage tolerance; impact; T-pull; delamination

1. Introduction

The typical aerospace applications of composite intersections include the use of I-Beams, T-joints and T-stiffeners (Stickler 2001). Prominent at locations where stiffeners attach to the wing skins, and where those wing skins attach to the ribs and other structural elements in the aircraft. It is at these interfaces where failures typically occur, in the form of delamination between the skin and the flange of the stiffened section (Bigaud 2018). Structural adhesives are sensitive to through-thickness, and peel stresses (Broughton 2002), and typical high temperature infusion resins

*Corresponding author, MEng., E-mail: Harry.Clegg@Bristol.ac.uk
[a] Ph.D., E-mail: Giuseppe.Dellanno@nccuk.com
[b] Ph.D., E-mail: I.K.Partridge@Bristol.ac.uk

http://www.techno-press.org/?journal=aas&subpage=7 ISSN: 2287-528X (Print), 2287-5271 (Online)

systems are even more sensitive to these out of plane loads.

With the growing demand for part count reduction, manufacturers are looking to explore methods which facilitate the co-infusion, and co-curing of these complex composite structures. This is driven by industry attempts to reduce costs in reducing the complexity of manual assembly required. The assembly of multiple preforms prior to infusion may in part realise this, however, the typically low resistance to delamination of traditional planar (2D) composites restricts the possibilities of integrating components (Partridge and Hallett 2016). A longstanding problem with T-joints is delamination cracking between the skin and the stiffener caused by out-of-plane loads, impact or environmental degradation (Bianchi 2012).

To combat the low resistance to delamination, composite structures are commonly fastened using bolts and rivets. The process of drilling and bolting locally destroys the load-bearing fibres and can introduce high local stresses into regions already weakened from severed fibres (Burns 2012). The current practice is to create back-to-back composite "L's" (Cullinan 2016), by the forming of plies around the radius between the flange and the web parts of the stiffened section, or intersection, and secondary bonding followed by mechanical fastening. The design of secondarily bonded joints must allow for the later mechanical fastening of the joint (Broughton 2002), and in some cases even facilitate later rework up to the next nominal size. In these cases, it is the adhesive that is transferring the load, the bolts only able to transfer the load after the initiation of failure in the adhesive. The mechanical fastening is then providing assurance that adhesive failures will not be allowed to propagate in an unstable manner.

The application of selective Through-Thickness Reinforcement to composites have been achieved in the form of tufting (Dell'Anno 2007), Z-pinning (Greenhalgh 2006) with models proposed (Allegri and Zhang 2007), or stitching (Dransfield and Baillie 1994), and has been associated with the benefits of the application of fibres in the through-thickness direction on the interlaminar, and out-of-plane properties (Partridge and Hallett 2016). These insertions are also with an associated with a reduction of the static in-plane properties (Mouritz 1997), fatigue properties (Mouritz 2010), and their own specific defect mechanisms (Scott *et al*. 2018). The application of selective Through-Thickness Reinforcement to stiffened composite structures has previously been suggested in the form of stitching (Greenhalgh 2003) and the pull off performance investigated (Bigaud 2018), the application of Z-pinning investigated (Vazquez 2011) and shown to increase the ultimate load in a pull of scenario (Koh 2012), the effect of tufting on the delamination propagation (Cartié 2006) and manufacturing methods suitable for the production of lab-scale elements detailed (Dell'Anno *et al*. 2016). Other models have been previously proposed for Z-pinned T's (Bianchi 2012), and the mechanical response and the bridging mechanisms of tufts investigated (Osmiani 2016). Other investigations have included the application of stitching for the improvement in the resistance to impact damage (Yoshimura 2008), the use of polymer threads for self-healing (Yang 2013), the effect of stitch density on damage progression (Tan 2013), and the use of tufted yarns for the structural health monitoring of a composite (Martins 2018).

Broad goods are commonly used to create the intersection of T-joints using back-to-back L's, an alternative to the cutting and forming of broad goods would be the utilisation of a 3D woven sub-preform to form the composite intersection (Tomblin 2017). This paper documents the investigation of the application of 3D woven sub-preforms and identifies a significant performance advantage when 3D woven sub-preforms are utilised to create these composite intersections, which have widespread application across multiple sectors. The effect of Tufting for the Through-Thickness Reinforcement of the intersection is also investigated, and the changes in mechanical performance and detailed.

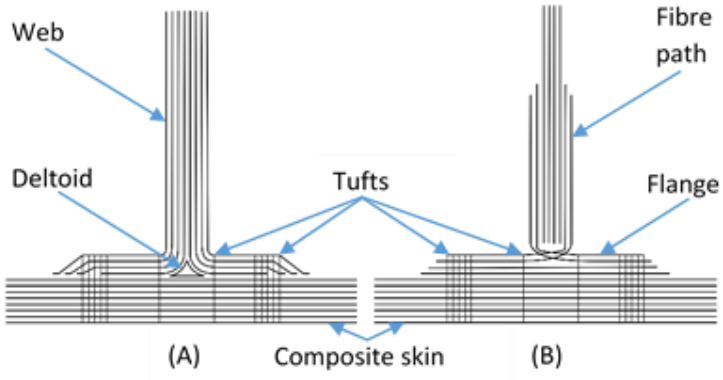

Fig. 1 Areas of selective application of Tufting at the flange transition, and bounding the noodle: (A) with back-to-back L's, (B) with the 3D woven π connector fibre architectures

2. Materials and methods

A Computer-Numeric-Controlled Ply cutter was used to cut the plies from broad goods, a 400 gsm Non-crimped T700 +45/-45 carbon fibre fabric. The back-to-back "L" sub preforms were assembled into a jig that facilitated the placement of the deltoid shape filler or "noodle". The deltoid shape was filled using multiple unbound T700 12K 50C carbon tows, with a 56% target fibre fill ratio, placed onto the preform with a jig to control the tension and alignment. The control specimens, using the both the back-to-back L's technique, and the 3D woven π connector were manufactured without tufting. Test specimens were also manufactured for each fibre architecture variant with tufting: To provide a comparison between both of the fibre architecture variations tested, and the effect of tufting for selective Through-Thickness Reinforcement on each of the fibre architectures in question. The 3D woven sub-preforms used in this study were manufactured by Sigmatex UK Ltd., using the same T700 12K tows. The fibre architecture of the 3D woven π section was balanced in the warp and weft direction, the flange element was made up of a four-layer orthogonal interlock weave. Two of the layers from the flange were passed upwards, intersected with their opposing layers from the opposite side of the flange and formed the webs. In the woven π-section, the areal density of fibres in the through-thickness direction was 5.47%.

2.1 Tufting

Through-Thickness Reinforcement represents a valid method for the reinforcement of structural joints (Dell'Anno *et al*. 2016). Previous studies have investigated the application of tufting in T-joints (Cartié et al. 2006). In this study, tufting was applied to selected areas of both the back-to-back "L", and the 3D woven π section preforms, using a KSL522 tufting head, in conjunction with a Kuka KR240 extended reach robotic arm. Tufts are applied at the transitions from the stiffener to the skin, and bounding the deltoid region as shown in Figure 1. The carbon thread utilised in this application is an industrially available 4*67 HTA40 thread from Schappe, France. The tufting patterns applied during this work were developed previously using mechanical testing on glass fibre epoxy composite T-sections (Kratz *et al*. 2015), the tufting application around the deltoid region was adopted from prior work (Clegg *et al*. 2016). The tufts were inserted through the full thickness of both the preform, and the stiffener flange, at an areal density of 3.4%.

2.2 Infusion and cure

The preforms used in this study were to be cured using a semi-rigid tooling section in conjunction with a flat plate tool and a semi-permeable membrane. The radii at the web locations are 10mm and 3mm, for the back-to-back L's and the 3D woven π forms respectively. The over laminate thickness' were 4mm in both cases. The taper at the flange to skin transition was 8.5°. The polymer selected for the infusion of the composite T-sections was an epoxy resin system, Epikote RIMR 135 resin, with RIMH 137 hardener - from Hexion, Germany. 100 parts (resin) to 30 (hardener) by weight. The preforms were removed from the preforming tool, including the removal of the consumable foam sections used during the tufting process. The preforms were then prepared for infusion with the application of consumable materials and tooling sections. The infusion was carried out at 50°C, at full vacuum. Cure was established by increasing the part temperature to 80°C, and dwelling for 2 hours. The resulting specimens were measured in multiple locations with a digital micrometer to allow for estimation of the fibre volume fraction: The control back-to-back L's specimens had an average fibre volume fraction of 57.9%, the tufted back to back L's an average of 56.9%, the control π-section an average of 56.1%, and the tufted π-section an average of 55.8%.

2.3 Specimen preparation

The manufactured composite T-section stiffened panels were then sectioned into coupons. A 30mm coupon width was selected to reduce the prevalence of edge effects, with a total width of 300mm centred about the stiffener. The specimens were extracted using an automated plate cutter, outfit with a diamond blade. Cooling, lubrication and dust removal were provided by a water feed inbuilt into the plate cutting machine. Surfaces were consistent after cutting, featuring minor striations from the diamond saw only, and no further finishing processes were performed. Specimens were prepared prior to test with a high contrast speckled pattern to allow tracking during test using a Digital Image Correlation (DIC) system.

2.4 Testing and analysis methodology

2.4.1 T-pull test setup

A T-pull test setup was implemented, with the lower fixture support pins at a distance of 250mm, centre to centre. The web of the T-section stiffened structures was clamped in the top jaw of the test machine. Sections were fixed into the top jaw, using a torque wrench to allow the specimens to be clamped consistently. The load pins were separated, and the skin laminate left unsupported to allow the creation of a complex load condition, with a combination of mode I opening, and mode II shear. During testing, a high through-thickness tension results due to the application of the tensile load through the web, and shear stresses are induced at the flange to skin transitions, caused by the bending deflection of the specimen under load. Tests were performed under displacement control at a crosshead velocity of 2mm/min. Force and displacement data were recorded whilst the DIC system tracked the local deformation. The DIC also provided a secondary external measurement of the induced displacement.

2.4.2 Impactor test setup

For the specimens which were selected for impact, a DynaTup 9250 drop weight impactor from Instron. The impactor setup utilised with a 12.2mm hemispherical impactor head, the impact

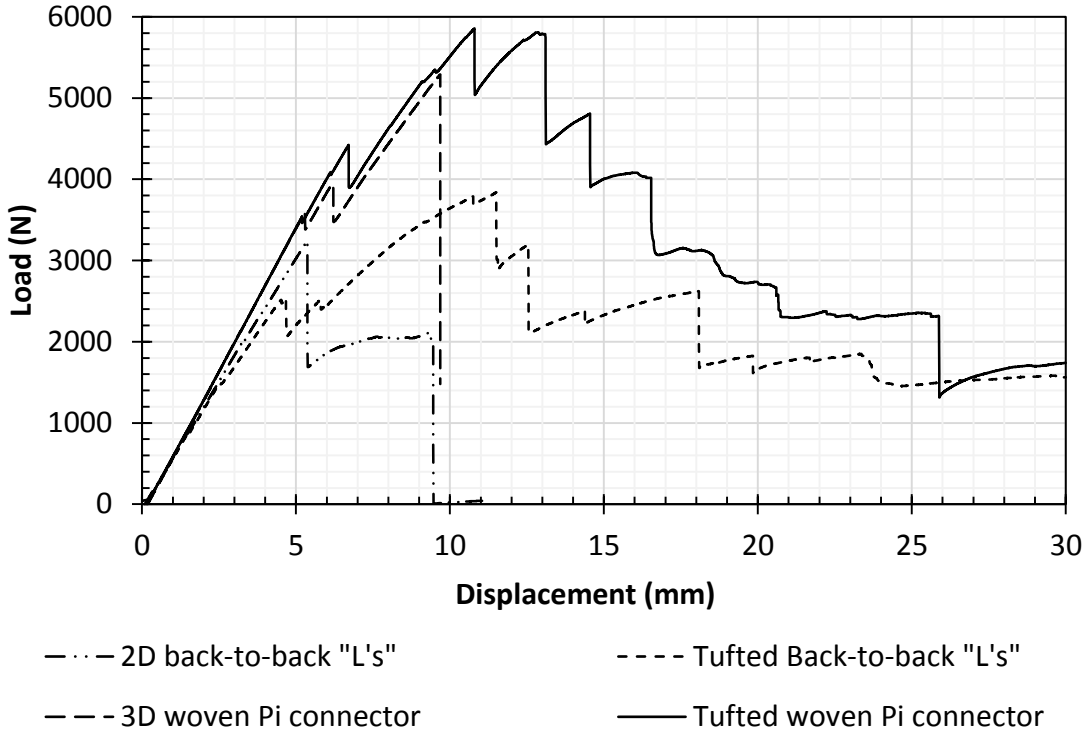

Fig. 2 Representative curves from mechanical test for intersections with back-to-back "L's", tufted back-to-back "L's", 3D woven π, and tufted 3D woven π

energy set using a fixed mass and height to obtain a 50J impact. The span of the specimen across the Dynatup base plate was 80mm, with the specimen positioned so that the impact event occurred on the skin side of the component, centrally within the specimen and directly underneath the web. The specimen was secured into place using mechanical clamps, and secondary impacts were prevented by the use of pneumatically actuated bump stops.

2.5 Analysis methodology

The outputs from the load cell were used along with the measured displacement to create load-displacement results for each configuration. This in turn was used to establish the apparent stiffness of each of the sections tested. During testing audible cracks were noted, corresponding to drops in the load trace, suggesting the onset of failure. The type of failure was also recorded, including the site of initiation of failure. The failures are categorised as stiffener-to-skin separation or fibre failure within the laminate, or a combination of both. It was also noted if the failure was symmetric, or asymmetric. The Digital Image Correlation system allows the development of the failure through each specimen to be examined thoroughly. The DIC system is also capable of tracking individual locations on the specimen during test, and compute from local displacements the local strain. The extension measured by the DIC system can be used to reduce the effect of test frame error on the force displacement curves.

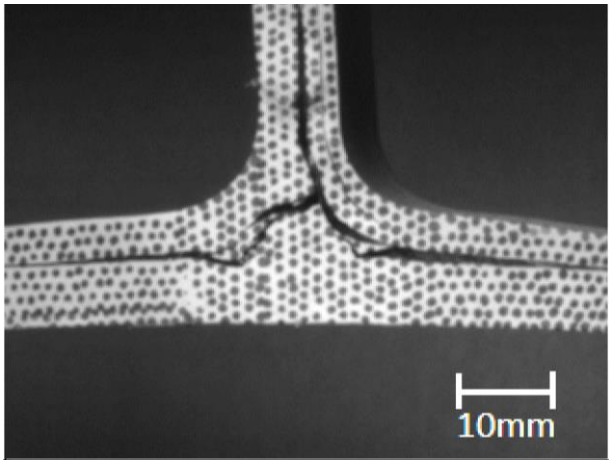

Fig. 3 Failure paths within the back-to-back L's configuration

3. Results and discussion

3.1 T-Pull testing of as manufactured specimens

The intersection configurations described previously were subject to mechanical test in a T-pull configuration, with specimens in an as manufactured condition. Indicative curves from each set of tests have been selected for comparison: The plot shown in Figure 2 is the load-displacement response for the composite T-section intersections with two dimensional, and three dimensional fibre architectures at the intersection, with and without selective reinforcement—as detailed in Figure 1—in the form of tufting.

The control configuration for this comparison is the 2D back-to-back L's. The specimen chosen to be representative of this configuration shows a reduction in load carrying ability of approximately 50% after the initiation of failure. The failure initiated in the deltoid region, and progressed outwards along the stiffener-to-skin interface as shown in Figure 3, and into the web before full failure was achieved by stiffener-to-skin separation.

The 2D back-to-back L's configuration can be compared the tufted back-to-back "L's" configuration, with the latter displaying an ability to carry further load after the initiation of failure at the deltoid. The tufted back-to-back "L's" surpasses the maximum load attained by the un-tufted counterpart, and continues to carry load until large displacements are reached. The failure is prevented from progressing outwards from the deltoid along the stiffener-to-skin interface by the presence of the tufts bounding the deltoid. A specimen of the tufted back-to-back L's is shown in Figure 4, after the initiation of failure in the deltoid with failure progressing from the deltoid, upwards into the web.

The final stage of failure when the deltoid is bounded by tufts changes from stiffener-to-skin separation to fibre failure in the skin laminate. Whilst corresponding to an increase in the area under curve, the change in failure mode may prove to be undesirable. The 3D woven connector displays an ability to carry load that exceeds the capabilities of the 2D back-to-back "L's". The initiation load for the 3D woven π connector is greater, the initiation of failure is shown in Figure 5. The failure initiates at the base of the web, between the 3D woven section and the non-crimped fabric skin. The structure continues to carry load up until a second peak, observed at near double

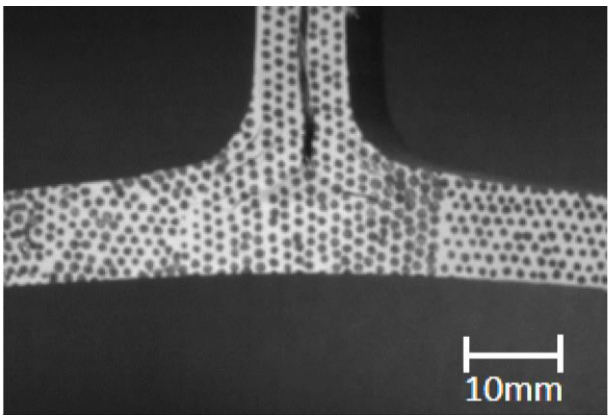

Fig. 4 A tufted back-to-back L's specimen during test, after the initiation of failure at the deltoid region, with failure progressing into the web

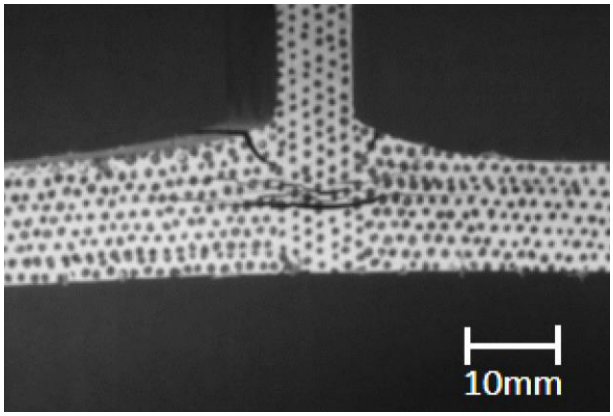

Fig. 5 The initiation of failure in the 3D woven π configuration, with failure initiating at the base of the web, between the 3D woven π and the non-crimped fabric skin

the load of the 2D back-to-back L's configuration. The final failure is in the form of stiffener-to-skin separation.

The 3D woven π connector, secured to the skin laminate using tufting shows similar behaviour of the un-tufted version, up until the 2nd peak, the maximum load achieved: After this the notable difference in the behaviour is the load carrying ability that it achieves, even until large displacements are reached. The developing final failure is shown in Figure 6, where the initiation of failure is at the base of the web, and further failure is seen in the form of fibre failure in the skin. The propagation of this final stage of failure can be observed in Figure 6, where the failure begins on the outer skin surface as buckling of the surface plies at the tufted locations and propagates inwards into the intersection.

3.2 T-Pull testing of impacted specimens

The intersection configurations described previously were subject to mechanical test in a T-pull configuration, with specimens in an impacted condition. Impacts were enacted onto the 3D π configuration specimens, with impacts enacted onto both the control, and tufted variants as

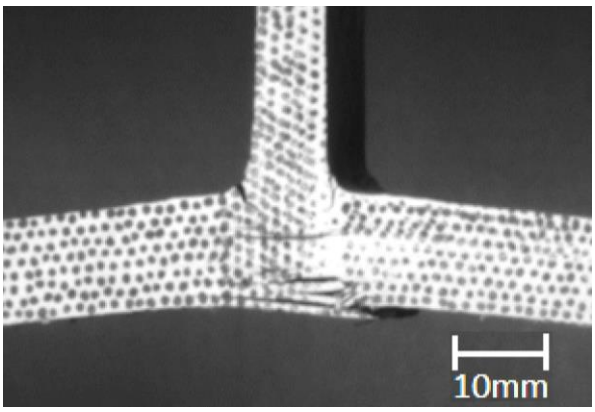

Fig. 6 The progression of failure in the tufted 3D woven π configuration, with failure initiating at the base of the web, the presence of tufts near the intersection between the 3D woven section and the Non-crimped fabric skin preventing propagation of failure along the stiffener-skin interface

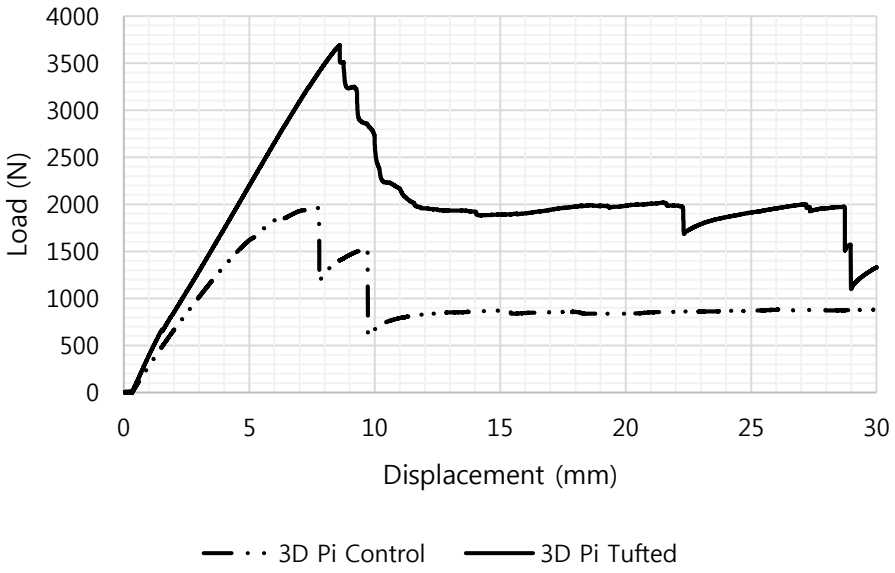

Fig. 7 Representative curves from mechanical test for intersections of the 3D woven π, and tufted 3D woven π configurations subject to a 50J impact to the skin side directly underneath the web

detailed in Section 2.1. Indicative curves from each set of tests after impact have been selected for comparison: The T-pull test setup used was identical to the setup described in Section 2.42.

Figure 7 shows representative curves obtained from the after impact T-pull testing. It can be observed that the peak load in both cases has been reduced by the impact event, the first failure having initiated during the impact event. The compliance of the specimen is thereby increased, and the load carrying ability decreased in both cases. The T-joint featuring a 3D woven π connector, with tufting applied according to the specification described in section 2.1, was shown to outperform the control in the after impact test, retaining a larger proportion of the as manufactured load carrying ability.

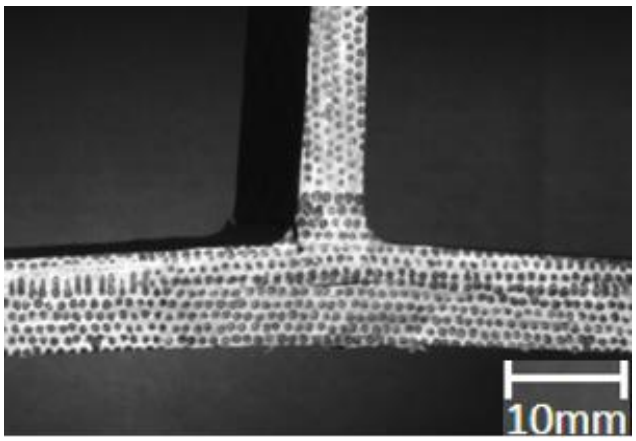

Fig. 8 The tufted 3D π specimen during the T-pull test, after being subject to a 50J impact on the skin side directly below the web: The first signs of failure already present

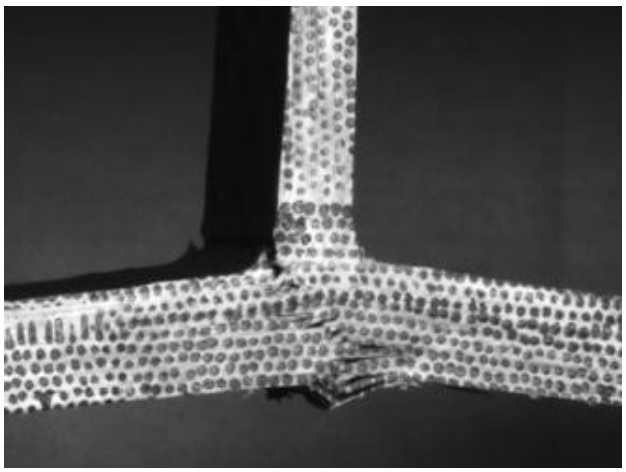

Fig. 9 The tufted 3D π specimen during the T-pull test, after being subject to a 50J impact on the skin side directly below the web: During the final stage of failure, which begins as fibre failure via ply buckling at the outer surface of the intersection on the skin side

The presence of delamination at the interface of the 3D woven π connector and the skin laminate can be observed in Figure 8. Without a notable drop in the load displacement trace, or audible cracking during test, the author stipulates that this failure—the delamination between the 3D woven π connector and the skin laminate—has initiated during the impact event. The propagation of this delamination is constrained by the presence of the tufts bounding the web region, however the failure is driven into a fibre failure dominated failure mode.

The propagation of this crack is prevented by the presence of the tufts bounding the impacted region, the failure mode observed was fibre failure of the skin laminate as shown in Figure 9. The retained portion of the load carrying ability in the tufted specimens is greater than that of the equivalent control specimens: The impact event appears to have initiated the failure of the specimen, and the load trace of the impacted specimens shows increased compliance and reduced load carrying ability.

4. Conclusions

A notable increase in the load bearing capacity can be obtained by the application of selective Through-Thickness Reinforcement in the form of tufting, to traditional 2D fibre architectures. Lower energy failure modes can be prevented, resulting in an increase in the post initiation section stiffness and load carrying ability, at the risk of driving the failure into a different mode, i.e. fibre failure within the skin laminate.

The use of 3D woven composite connectors has been demonstrated to simplify manufacturing processes, removing a portion of time associated with the forming of back-to-back "L's". This is advantageous in a manufacturing environment, where takt time accounts for a significant portion of the cost of the manufactured part.

The mechanical performance of 3D woven connectors is superior to that of those created using 2D materials by 57%. The properties of 3D woven structures are often considered to be inferior to those of planar, 2D composites: This work demonstrates that when utilised properly, 3D woven structures are able to out-perform their 2D equivalents. The removal of the deltoid or noodle region by the adoption of a 3D woven π connector also eliminates the stress concentrator that is associated with it. The interlaminar tension that is produced by the resin-dominated shrinkage of the deltoid region is minimised, and as such, the as-manufactured performance of the structure is improved.

The addition of tufting appears in this case not to affect the initiation load of either the 2D tufted, or the 3D woven π in this case, however a significant increase in the residual load carrying ability of the structure is demonstrated when an out-of-plane load is applied, denoted by the increasing load required to continue the propagation of failure. In the case where a 3D woven π connector is used in conjunction with tufting, the ultimate load can be increased by up to 82% in comparison to the 2D fibre architecture back-to-back L's examples.

The application of tufting to the regions immediately bounding the web cause a change in failure mode from stringer skin separation, to fibre failure in the skin plies. It is stipulated that if tufting was applied only to the stiffener to skin transition, then the failure mode would not be changed to fibre failure of the skin laminate: But remain as a form of stiffener and skin separation, and still increasing the load carrying ability of the structure. To avoid fibre dominated failure modes in pull off scenarios, the application of tufting should be avoided in the region immediately bounding the web, and should instead be focused on the stiffener flange to skin transition areas.

Acknowledgements

This work was supported by the National Composites Centre Core Research and Technology Programmes (www.nccuk.com). The authors would like to acknowledge the support of the Engineering and Physical Sciences Research Council through the EPSRC Centre for Doctoral Training in Composites Manufacture [EP/K50323X/1].

References

Allegri, G. and Zhang, X. (2007), "On the delamination suppression in structural joints by Z-fibre pinning", *Compos. Part A Appl. Sci. Manufact.*, **38**, 1107-1115

Bianchi, F. (2012), "Finite element modelling of Z-pinned composite T-joints", *Compos. Sci. Technol.*, **73**, 48-56.
Bigaud, J. (2018), "Analysis of the mechanical behaviour of composite T-joints reinforced by one sided stitching", *Compos. Struct.*, **184**, 249-255.
Broughton, W.R. (2002), "Design requirements for bonded and bolted composite structures", *NPL Report MATC(A)65*; National Physical Laboratory, United Kingdom.
Burns, L. (2012), "Bio-inspired design of aerospace composite joints for improved damage tolerance", *Compos. Struct.*, **94**(3), 995-1004.
Cartié, D.D.R. (2006), "3D reinforcement of stiffener-to-skin t-joints by z-pinning and tufting", *Eng. Fracture Mech.*, **73**(16), 2532-2540.
Clegg, H.M., Kratz, J.K., Partridge, I.K. and Dell'Anno, G. (2016), "Evaluation of the effects of tufting on performance of composite T-joints", *Proceedings of the 17th European Conference on Composite Materials*, June, Munich.
Cullinan, J.F. (2016), "Damage manipulation and in situ repair of composite T-joints", *J. Aircraft*, **53**, 1013-1021.
Dell'Anno, G., Treiber, J.W.G. and Partridge, I.K. (2016), "Manufacturing of parts reinforced through-thickness by tufting", *Robotics Comput.-Integrated Manufact.*, **37**, 262-272.
Dell'Anno, G. (2007), "Effect of tufting on the mechanical behaviour of carbon fabric epoxy composites", Ph. D. Dissertation, Cranfield University, United Kingdom.
Dransfield, K. and Baillie, C. (1994), "Improving the delamination resistance of CFRP by stitching – A review", *Compos. Sci. Technol.*, **50**(3), 305-317.
Greenhalgh, E. (2003), "The assessment of novel materials and processes for the impact tolerant design of stiffened composite aerospace structures", *Compos. Part A*, **34**, 151-161.
Greenhalgh, E.S. (2006), "Evaluation of toughening concepts at structural features in CFRP Part I: Stiffener pull-off", *Compos. Part A*, **37**, 1521-1535.
Kratz, J., Clegg, H.M., Dell'Anno, G. and Partridge, I.K. (2015), "Improving the damage tolerance of composite joints with tufting", *Proceedings of the 20th International Conference on Composite Materials*, July, Copenhagen.
Martins, A.T. (2019), "Structural health monitoring for GFRP composite by the piezoresistive response in the tufted reinforcements", *Compos. Struct.*, **209**, 103-111.
Mouritz, A.P. (1997), "A review of the effect of stitching on the in-plane mechanical properties of fibre-reinforced polymer composites", *Compos. Part A*, **28**, 979-991.
Mouritz, A.P. (2010), "Design dilemma for Z-pinned composite structures", *27th International Congress of the Aeronautical Sciences 2010*, September, Nice.
Osmiani, C. (2016), "Exploring the influence of micro-structure on the mechanical properties and crack bridging mechanisms of fibrous tufts", *Compos. Part A*, **91**, 409-419.
Partridge, I.K. and Hallett, S.R. (2016), "Use of microfasteners to produce damage tolerant composite structures", *Philos. T. R. Soc. A*, **374**, 20150277.
Scott, M., Dell'Anno, G. and Clegg, H.M. (2018), "Effect of process parameters on the geometry of composite parts reinforced by through-the-thickness tufting", *Appl. Compos. Mater.*, **25**(4), 785-796.
Stickler, P.B. (2001), "Investigation of mechanical behaviour of transverse stitched T-joints with PR520 resin in flexure and tension", *Compos. Struct.*, **52**(3-4), 307-314.
Tan, K.T. (2013), "Effect of stitch density and stitch thread thickness on damage progression and failure characteristics of stitched composites under out-of-plane loading", *Compos. Sci. Technol.*, **74**, 194-204.
Tomblin, J.S. and Salah, L. (2017), "Teardown evaluation of a composite carbon epoxy beechcraft starship aft wing", DOT/FAA/TC-15/47; Federal Aviation Administration, William J. Hughes Technical Center, Aviation Research Division, Atlantic City, U.S.A.
Vazquez, J.T. (2011), "Multi-level analysis of low-cost Z-pinned composite joints part 1: Single Z-pin behaviour", *Compos. Part A*, **42**, 2070-2081.
Yang, T. (2013), "Healing of carbon fibre-epoxy composite T-joints using mendable polymer fibre stitching", *Compos. Part B*, **45**, 1499-1507.

Yoshimura, A. (2008), "Improvement of out-of-plane impact damage resistance of CFRP due to through-the-thickness stitching", *Adv. Compos. Mater.*, **18**(2), 121-134.

CC